Measurement of CP Violation in $B^0 \to J/\psi K^0_S$ Decays

R. Aaij *et al.*[*]
(LHCb collaboration)

(Received 25 March 2015; published 14 July 2015)

Measurements are presented of the CP violation observables S and C in the decays of B^0 and $\bar{B}^0$ mesons to the $J/\psi K^0_S$ final state. The data sample corresponds to an integrated luminosity of 3.0 fb^{-1} collected with the LHCb experiment in proton-proton collisions at center-of-mass energies of 7 and 8 TeV, and contains a total of 41 560 selected B^0 and $\bar{B}^0$ decays. The analysis of the time evolution of these decays yields $S = 0.731 \pm 0.035(\text{stat}) \pm 0.020(\text{syst})$ and $C = -0.038 \pm 0.032(\text{stat}) \pm 0.005(\text{syst})$. In the standard model, S equals $\sin(2\beta)$ to a good level of precision. The values are consistent with the current world averages and with the standard model expectations.

DOI: 10.1103/PhysRevLett.115.031601 PACS numbers: 11.30.Er, 12.15.Hh, 13.25.Hw

The violation of charge-parity (CP) conservation in processes involving B mesons was first observed in the "golden mode" $B^0 \to J/\psi K^0_S$ by the *BABAR* and Belle experiments at the asymmetric e^+e^- colliders PEP-II and KEKB [1,2]. Since then, measurements of CP violation in this decay mode have reached a precision at the level of 10^{-2} [3,4]. Thus, these measurements play an important role in constraining and testing the quark-flavor sector of the standard model [5,6], which relates CP-violating observables to a single irreducible phase in the Cabibbo-Kobayashi-Maskawa (CKM) quark-mixing matrix [7,8]. As the $J/\psi K^0_S$ final state is common to both the B^0 and the $\bar{B}^0$ meson decays, the interference between the amplitudes for the direct decay and for the decay after B^0-$\bar{B}^0$ oscillation results in a decay-time dependent CP asymmetry between the time-dependent decay rates of B^0 and $\bar{B}^0$ mesons

$$\mathcal{A}(t) \equiv \frac{\Gamma(\bar{B}^0(t) \to J/\psi K^0_S) - \Gamma(B^0(t) \to J/\psi K^0_S)}{\Gamma(\bar{B}^0(t) \to J/\psi K^0_S) + \Gamma(B^0(t) \to J/\psi K^0_S)} = \frac{S\sin(\Delta m t) - C\cos(\Delta m t)}{\cosh(\frac{\Delta\Gamma t}{2}) + A_{\Delta\Gamma}\sinh(\frac{\Delta\Gamma t}{2})}. \quad (1)$$

Here, $B^0(t)$ and $\bar{B}^0(t)$ indicate the flavor of the B meson at production, while t indicates the decay time. The parameters Δm and $\Delta\Gamma$ are the mass and the decay width differences between the heavy and light mass eigenstates of the B^0-$\bar{B}^0$ system, and S, C, and $A_{\Delta\Gamma}$ are CP observables. As $\Delta\Gamma$ is negligible for the B^0-$\bar{B}^0$ system [9], the time-dependent asymmetry simplifies to $\mathcal{A}(t) = S\sin(\Delta m t) - C\cos(\Delta m t)$.

The $B^0 \to J/\psi K^0_S$ decay is dominated by a $\bar{b} \to c\bar{c}\,\bar{s}$ transition, and CP violation in the decay is expected to be negligible at the current level of experimental precision, giving $C \approx 0$. (Mention of a particular decay mode implies the inclusion of charge-conjugate states except when the measurement of CP violation is involved.) This allows us to identify S with $\sin(2\beta)$, where $\beta \equiv \arg[-(V_{cd}V^*_{cb})/(V_{td}V^*_{tb})]$ is one of the angles of the CKM triangle. Other measurements that constrain this triangle predict $\sin(2\beta)$ as $0.771^{+0.017}_{-0.041}$ [10], giving a small discrepancy with respect to the average of direct measurements, 0.682 ± 0.019 [9], where the most precise input comes from a CP violation measurement in $B^0 \to J/\psi K^0_S$ decays by the Belle experiment, $S = 0.670 \pm 0.029(\text{stat}) \pm 0.013(\text{syst})$ [4]. To clarify the CKM picture, both better experimental precision and improved understanding of higher-order contributions to the decay amplitudes are required [11,12].

The analysis presented in this Letter supersedes a previous measurement by LHCb [13], which was performed on data corresponding to an integrated luminosity of 1.0 fb^{-1} at a center-of-mass energy of 7 TeV. By adding data corresponding to 2 fb^{-1} at 8 TeV and using an optimized selection and additional "flavor tagging" algorithms to identify the quark content of the B meson at production, we increase the statistical power of the analysis by almost a factor 6.

The LHCb detector [14,15] is a single-arm forward spectrometer covering the pseudorapidity range $2 < \eta < 5$, designed for the study of particles containing b or c quarks. The detector includes a high-precision tracking system consisting of a silicon-strip vertex detector surrounding the pp interaction region, a large-area silicon-strip detector located upstream of a dipole magnet, and three stations of silicon-strip detectors and straw drift tubes placed downstream of the magnet. Different types of charged hadrons are distinguished using information from two ring-imaging Cherenkov detectors. Photon, electron, and

[*]Full author list given at the end of the article.

hadron candidates are identified by a calorimeter system consisting of scintillating-pad and preshower detectors, an electromagnetic calorimeter, and a hadronic calorimeter. Muons are identified by a system composed of alternating layers of iron and multiwire proportional chambers. The online event selection system (trigger) [16] consists of a hardware stage, based on information from the calorimeter and muon systems, followed by a software stage.

The analysis is performed with $B^0 \to J/\psi K^0_S$ candidates reconstructed in the $J/\psi \to \mu^+\mu^-$ and $K^0_S \to \pi^+\pi^-$ final states. Two oppositely charged particles, identified as muons with high momentum and high transverse momentum, are required to originate from a common space point (vertex) and to have an invariant mass in a range ± 60 MeV$/c^2$ around the known J/ψ mass [17]. Since the B^0 meson has a lifetime of 1.5 ps and has high momentum, the resulting J/ψ candidate is required to be significantly separated from all reconstructed pp collision points [primary vertices (PVs)], of which there are on average 2.4 per event. The K^0_S candidates are formed from two oppositely charged, high-momentum pion candidates with a clear separation from any PV in the event. Candidates decaying early enough for the final-state pions to be reconstructed in the vertex detector are characterized as long candidates and are required to have an invariant mass within ± 15 MeV$/c^2$ of the known K^0_S mass [17]. The K^0_S candidates that decay later, such that track segments of the pions cannot be formed in the vertex detector, are called downstream candidates; these have a poorer momentum resolution than the long candidates, and thus the corresponding $\pi^+\pi^-$ pairs are required to have an invariant mass within ± 55 MeV$/c^2$ of the known K^0_S mass. A good vertex fit quality and sufficient separation from the B^0 decay vertex are required for the K^0_S candidate's decay vertex. To reduce background contributions from $\Lambda^0_b \to J/\psi\Lambda$ decays, the π^+ (π^-) candidate has to fulfill particle identification requirements if the invariant mass under a $p\pi^-$ ($\pi^+\bar{p}$) mass hypothesis is compatible with the Λ mass.

The B^0 candidates are reconstructed from J/ψ and K^0_S candidates that form a good quality vertex. Multiple PVs and, in a small fraction of events, multiple $B^0 \to J/\psi K^0_S$ candidates, lead to multiple (B^0, PV) pairs per event. For each pair, the decay time t is obtained from a fit to the full decay chain while constraining the production vertex of the B^0 candidate to the respective PV [18]. The reconstructed B^0 candidate mass m is obtained from a similar fit with the $\mu^+\mu^-$ and $\pi^+\pi^-$ invariant masses constrained to the known J/ψ and K^0_S masses. The latter fit must satisfy loose requirements on its quality, and resulting candidates are only retained if $5230 < m < 5330$ MeV$/c^2$ and $0.3 < t < 18.3$ ps. The fit uncertainty σ_t on the decay time is required to be smaller than 200 fs, which is well above the average resolution of 55 fs (65 fs) for candidates with long (downstream) K^0_S daughters. The quantity σ_t is used later in the analysis as an estimate of the per-candidate decay-time resolution. In events where more than one (B^0, PV) pair satisfies all selection requirements, one is chosen at random.

Various simulated data samples are used in the analysis. In the simulation, pp collisions are generated using PYTHIA [19] with a specific LHCb configuration [20]. Decays of hadronic particles are described by EVTGEN [21]. The interaction of the generated particles with the detector, and its response, are implemented using the GEANT4 toolkit [22] as described in Ref. [23].

Tagging algorithms are used to infer the initial flavor of the B meson candidate, i.e., whether it contained a b or a $\bar{b}$ quark at production. Each algorithm provides a decision d on the flavor of the B meson candidate (tag), and an estimate η of the probability for that decision to be incorrect (mistag probability). The knowledge of the B meson production flavor is essential for this analysis, and so only candidates for which the tagging algorithms yield a decision are considered.

One class of flavor tagging algorithms, the opposite-side (OS) tagger, exploits the dominant production mechanism of b hadrons, i.e., the production of $b\bar{b}$ quark pairs, by reconstructing the b hadron produced in association with the signal B meson. The OS tagger uses the charge of the electron or muon from semileptonic b decays, the charge of the kaon from the $b \to c \to s$ decay chain, and the inclusive charge of particles associated with the secondary vertex reconstructed from the b hadron decay products; further details are described in Ref. [24].

A major improvement in this analysis over Ref. [13] is the inclusion of the same-side pion (SSπ) tagger, which deduces the production flavor by exploiting pions produced in the fragmentation of the b quark that produced the signal B meson or in the decay of excited B mesons into the signal B meson [25,26]. Tagging pion candidates are selected requiring charged, high momentum, and high transverse-momentum particles that are consistent with originating from the associated PV. Pions are identified using information from the particle identification detectors, and the difference between the invariant mass of the B and the $B\pi^\pm$ pair is required to be less than 1.2 GeV$/c^2$. Additionally, the flight directions of the pion and the B candidate must be compatible. If multiple pion candidates pass the selection, the one with the highest transverse momentum is used. The mistag probability is obtained using a neural network that is trained on simulated events and whose inputs are global event properties and kinematic and geometric information on the pion and B signal candidates.

The tagging calibration is performed in control samples of B mesons whose final state determines the B flavor at decay time, by determining a linear correction $\omega(\eta)$ that

relates the estimated mistag probability η with the mistag probability ω observed in the control sample. To account for asymmetries in the detection efficiency of charged particles, which can lead to different mistag probabilities for B^0 and $\bar{B}^0$ mesons, an additional linear correction function $\Delta\omega(\eta)$ is determined. Asymmetries in the efficiency of the algorithms in determining a decision are found to be negligible.

The $B^+ \to J/\psi K^+$ decay is used to determine the flavor tagging calibration for the OS tagger. A consistency check of the calibration is performed in a control sample of $B^0 \to J/\psi K^{*0}$ decays, showing a good correspondence of the calibration between B^+ and B^0 decays. As the quarks that accompany the b quark in B^+ and B^0 mesons differ, the SSπ tagger calibration is performed with $B^0 \to J/\psi K^{*0}$ decays [27]. Systematic uncertainties are assigned for the uncertainties associated with the calibration method and for the validity of the calibration in the signal decay mode. A summary of the calibration results is given in Ref. [28].

The effective tagging efficiency is the product of the probability for reaching a tagging decision, $\varepsilon_{\text{tag}} = (36.54 \pm 0.14)\%$, and the square of the effective dilution $D \equiv 1 - 2\omega = (28.75 \pm 0.24)\%$, which corresponds to an effective mistag probability of $\omega = (35.62 \pm 0.12)\%$. Compared to the previous LHCb analysis [13] the effective tagging efficiency $\varepsilon_{\text{eff}} = \varepsilon_{\text{tag}} D^2$ increases from 2.38% to 3.02%, mainly due to the inclusion of the SSπ tagger.

The values of the CP violation observables S and C are estimated by maximizing the likelihood of a probability density function (PDF) describing the unbinned distributions of the following observables: the reconstructed mass m, the decay time t and its uncertainty estimate σ_t, the OS and SSπ flavor tag decisions d_{OS} and $d_{\text{SS}\pi}$, and the corresponding per-candidate mistag probability estimates η_{OS} and $\eta_{\text{SS}\pi}$. The fit is performed simultaneously in 24 independent subsamples, chosen according to data-taking conditions (7 TeV, 8 TeV), K^0_S type (downstream, long), flavor tagging algorithm (OS only, SSπ only, OS and SSπ), and two trigger requirements. In each category the data distribution is modeled using a sum of two individual PDFs, one for the B^0 signal and one for the combinatorial background.

The reconstructed mass of the signal component is parametrized with a double-sided Hypatia PDF [29] with tail parameters determined from simulation. An exponential function is used to model the background component, with independent parameters for the downstream and long K^0_S subsamples. The fit to the mass distributions yields 41560 ± 270 tagged $B^0 \to J/\psi K^0_S$ signal decays. The mass distribution and projections of the PDFs are shown in Fig. 1(a).

The decay-time resolution is modeled by a sum of three Gaussian functions with common mean, but different widths, which are convolved with the PDFs describing the decay-time distributions. Two of the widths are given by the per-candidate resolution estimate σ_t, each calibrated with independent linear calibration functions. The third Gaussian describes the resolution for candidates associated with a wrong PV. The scale and width parameters are obtained in a fit to the decay-time distribution of a control sample of B^0 candidates formed from prompt J/ψ and K^0_S mesons. The parameters are determined separately for candidates formed from downstream and long K^0_S candidates.

Trigger, reconstruction, and selection criteria distort the measured B^0 decay-time distribution, leading to a decay-time dependent efficiency. Effects of the trigger requirements, which distort the decay-time distribution at low decay times, are determined using data and following the strategy used in Ref. [30]. The misreconstruction of tracks leads to inefficiencies at large decay times. To account for this effect, an additional decay-time dependent efficiency of the form $e^{-\beta_t t}$ is used, where β_t is obtained from simulation.

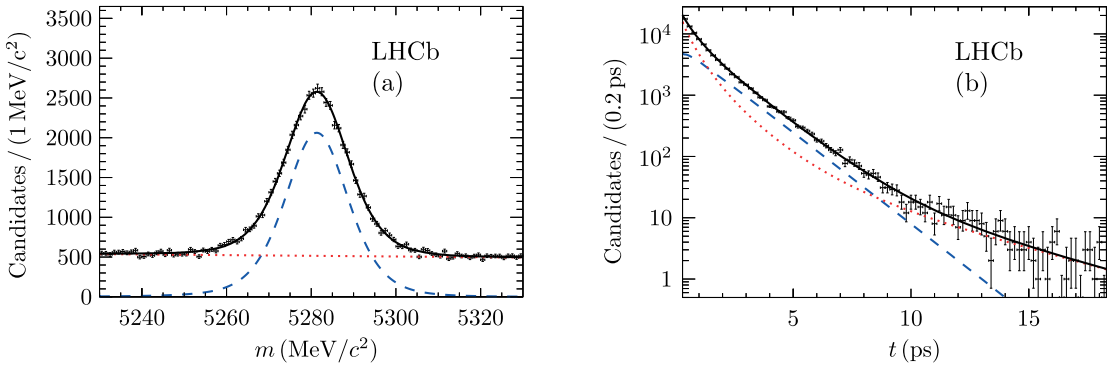

FIG. 1 (color online). (a) Distribution of the reconstructed mass and (b) logarithmic distribution of the decay time of tagged $B^0 \to J/\psi K^0_S$ candidates. The solid black lines show the fit projections, while the dashed (dotted) lines show the projections for the signal (background) components only.

The PDF of true decay times t' is given by

$$\mathcal{P}(t', d_{\rm OS}, d_{{\rm SS}\pi}|\eta_{\rm OS}, \eta_{{\rm SS}\pi}) = \sum_{d'}\left[\prod_j \zeta(d_j, \eta_j, d')\right](1 - d'A_P)e^{-t'/\tau} \times \{1 - d'S\sin(\Delta m t') + d'C\cos(\Delta m t')\}, \quad (2)$$

where the tag decision d takes the value $+1$ (-1) for a tagged B^0 ($\bar{B}^0$) candidate and d' takes the value $+1$ (-1) for the B^0 ($\bar{B}^0$) component of the signal distribution, τ is the B^0 meson lifetime, and

$$\zeta(d_j, \eta_j, d') = 1 + d_j\left\{1 - 2\left[\omega(\eta_j) + d'\frac{\Delta\omega(\eta_j)}{2}\right]\right\} \quad (3)$$

represents the calibration of the tagging response from the tagging algorithm $j = \{{\rm OS}, {\rm SS}\pi\}$. The production asymmetry $A_P \equiv [\sigma(\bar{B}^0) - \sigma(B^0)]/[\sigma(\bar{B}^0) + \sigma(B^0)]$, where σ denotes the production cross section inside the LHCb acceptance, is obtained using a measurement in 7 TeV pp collisions [31]. Considering differences between the 7 and 8 TeV data-taking conditions, the production asymmetries are determined as $A_P^{7\,\rm TeV} = -0.0108 \pm 0.0052({\rm stat}) \pm 0.0014({\rm syst})$ and $A_P^{8\,\rm TeV} = A_P^{7\,\rm TeV} + \Delta A_P$ with $\Delta A_P = 0.0004 \pm 0.0018({\rm syst})$ [32]. The background decay-time distribution is parametrized by a sum of exponential functions, convolved with the resolution model used for the signal. This parametrization does not depend on the tag decision and mistag probability estimates. The number of required exponential functions varies across subsamples. The decay-time distribution and projections of the PDFs are shown in 1(b). The distributions of the per-candidate resolution estimate σ_t and the per-candidate mistag probabilities, $\eta_{\rm OS}$ and $\eta_{{\rm SS}\pi}$, are modeled by empirical functions. Independent parameterizations are chosen for the signal and background components.

The likelihood is a function of 83 free parameters, including S and C, and 48 yield parameters for the signal and the background components in 24 individual subsamples. Eleven parameters are external inputs, including the production asymmetry, the flavor tagging calibration parameters, and the mass difference Δm [17]. These are constrained in the fit within their statistical uncertainties, taking their correlations into account. The likelihood fit yields $S = 0.729 \pm 0.035$ and $C = -0.033 \pm 0.032$ with a correlation coefficient of $\rho(S, C) = 0.483$. Figure 2 shows the decay time–dependent signal-yield asymmetry. An additional fit with fixed $C = 0$ yields $S = 0.746 \pm 0.030$. Corrections of $+0.002$ for S and -0.005 for C are applied to account for CP violation in $K^0 - \bar{K}^0$ mixing and for the difference in the nuclear cross sections in material between K^0 and $\bar{K}^0$ states [34]. The correction is negligible for the result for S with $C = 0$.

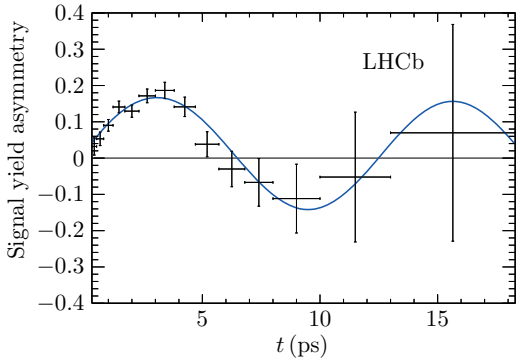

FIG. 2 (color online). Time-dependent signal-yield asymmetry $(N_{\bar{B}^0} - N_{B^0})/(N_{\bar{B}^0} + N_{B^0})$. Here, N_{B^0} ($N_{\bar{B}^0}$) is the number of $B^0 \to J/\psi K^0_S$ decays with a B^0 ($\bar{B}^0$) flavor tag. The data points are obtained with the *sPlot* technique [33], assigning signal weights to the events based on a fit to the reconstructed mass distribution. The solid curve is the projection of the signal PDF.

Various sources of systematic uncertainties on the CP observables are examined, in particular from mismodeling PDFs and from systematic uncertainties on the input parameters. In each study, a large set of pseudoexperiments is simulated using a PDF modified such as to include the systematic effect of interest; the relevant distributions from these pseudoexperiments are then fitted with the nominal PDF. Significant average deviations of the fit results from the input values are used as estimates of systematic uncertainties. The largest systematic uncertainty on S, ± 0.018, accounts for possible tag asymmetries in the background; for C the largest uncertainty, ± 0.0034, results from the systematic uncertainty on Δm. Systematic uncertainties on the flavor tagging calibration account for the second largest systematic uncertainty on S, ± 0.006, and on C, ± 0.0024. The third largest uncertainty on S, ± 0.005, arises from assuming $\Delta\Gamma = 0$ and is evaluated by generating pseudoexperiments with $\Delta\Gamma$ set to the value of its current uncertainty, 0.007 ps^{-1} [9], and then neglecting it in the fit. Remaining uncertainties due to neglecting correlations between the reconstructed mass and decay time of the candidates, mismodeling of the decay-time resolution and efficiency, the systematic uncertainty of the production asymmetry, and the uncertainty on the length scale of the vertex detector are small and are given in Ref. [28]. Adding all contributions in quadrature results in total systematic uncertainties of ± 0.020 on S and ± 0.005 on C.

Several consistency checks are performed by splitting the data set according to different data-taking conditions, tagging algorithms, and different reconstruction and trigger requirements. All results show good agreement with the nominal results.

In conclusion, a measurement of CP violation in the interference between the direct decay and the decay after B^0-$\bar{B}^0$ oscillation to a $J/\psi K^0_S$ final state is performed using 41 560 flavor-tagged $B^0 \to J/\psi K^0_S$ decays reconstructed with the LHCb detector in a sample of proton-proton

collisions at center-of-mass energies of 7 and 8 TeV, corresponding to an integrated luminosity of 3.0 fb^{-1}. The CP observables S and C, which allow the determination of the CKM angle β, are measured to be

$$S = 0.731 \pm 0.035(\text{stat}) \pm 0.020(\text{syst}),$$
$$C = -0.038 \pm 0.032(\text{stat}) \pm 0.005(\text{syst})$$

with a statistical correlation coefficient $\rho(S, C) = 0.483$. When C is fixed to zero the measurement yields $S = \sin(2\beta) = 0.746 \pm 0.030(\text{stat})$. This measurement supersedes the previous LHCb result obtained with 1.0 fb^{-1} [13], and represents the most precise time-dependent CP violation measurement at a hadron collider to date. Furthermore, the result has a similar precision to, and is in good agreement with, previous measurements performed at the Belle and *BABAR* experiments at the KEKB and PEP-II colliders [3,4]. This result is in excellent agreement with the expectations from other CKM related measurements and, after averaging with other results, improves the consistency of the CKM sector of the standard model.

We express our gratitude to our colleagues in the CERN accelerator departments for the excellent performance of the LHC. We thank the technical and administrative staff at the LHCb institutes. We acknowledge support from CERN and from the national agencies: CAPES, CNPq, FAPERJ, and FINEP (Brazil); NSFC (China); CNRS/IN2P3 (France); BMBF, DFG, HGF, and MPG (Germany); INFN (Italy); FOM and NWO (The Netherlands); MNiSW and NCN (Poland); MEN/IFA (Romania); MinES and FANO (Russia); MinECo (Spain); SNSF and SER (Switzerland); NASU (Ukraine); STFC (United Kingdom); NSF (USA). The Tier1 computing centers are supported by IN2P3 (France), KIT and BMBF (Germany), INFN (Italy), NWO and SURF (The Netherlands), PIC (Spain), and GridPP (United Kingdom). We are indebted to the communities behind the multiple open source software packages on which we depend. We are also thankful for the computing resources and the access to software research and development tools provided by Yandex LLC (Russia). Individual groups or members have received support from EPLANET, Marie Skłodowska-Curie Actions, and ERC (European Union), Conseil général de Haute-Savoie, Labex ENIGMASS, and OCEVU, Région Auvergne (France), RFBR (Russia), XuntaGal and GENCAT (Spain), Royal Society and Royal Commission for the Exhibition of 1851 (United Kingdom).

[1] B. Aubert *et al.* (*BABAR* Collaboration), Observation of CP Violation in the B^0 Meson System, Phys. Rev. Lett. **87**, 091801 (2001).

[2] K. Abe *et al.* (Belle Collaboration), Observation of Large CP Violation in the Neutral B Meson System, Phys. Rev. Lett. **87**, 091802 (2001).

[3] B. Aubert *et al.* (*BABAR* Collaboration), Measurement of time-dependent CP asymmetry in $B^0 \to c\bar{c}K^{(*)0}$ decays, Phys. Rev. D **79**, 072009 (2009).

[4] I. Adachi *et al.* (Belle Collaboration), Precise Measurement of the CP Violation Parameter $\sin 2\phi_1$ in $B^0 \to (c\bar{c})K^0$ Decays, Phys. Rev. Lett. **108**, 171802 (2012).

[5] A. B. Carter and A. I. Sanda, CP violation in B meson decays, Phys. Rev. D **23**, 1567 (1981).

[6] I. I. Y. Bigi and A. I. Sanda, Notes on the observability of CP violations in B decays, Nucl. Phys. **B193**, 85 (1981).

[7] N. Cabibbo, Unitary Symmetry and Leptonic Decays, Phys. Rev. Lett. **10**, 531 (1963).

[8] M. Kobayashi and T. Maskawa, CP violation in the renormalizable theory of weak interaction, Prog. Theor. Phys. **49**, 652 (1973).

[9] Y. Amhis *et al.* (Heavy Flavor Averaging Group), Averages of b-hadron, c-hadron, and τ-lepton properties as of summer 2014, arXiv:1412.7515. Updated results and plots are available at http://www.slac.stanford.edu/xorg/hfag/.

[10] J. Charles *et al.*, Current status of the standard model CKM fit and constraints on $\Delta F = 2$ new physics, Phys. Rev. D **91**. 073007 (2015).

[11] R. Aaij *et al.* (LHCb Collaboration) Measurement of the time-dependent CP asymmetries in $B_s^0 \to J/\psi K_S^0$, J. High Energy Phys. 06 (2015) 131; Measurement of the CP-violating phase β in $B^0 \to J/\psi\pi^+\pi^-$ decays and limits on penguin effects, Phys. Lett. B **742**, 38 (2015).

[12] K. De Bruyn and R. Fleischer, A roadmap to control penguin effects in $B_d^0 \to J/\psi K_S^0$ and $B_s^0 \to J/\psi\phi$, J. High Energy Phys. 03 (2015) 145; P. Frings, U. Nierste, and M. Wiebusch, Penguin contributions to CP phases in $B_{d,s}$ decays to charmonium, arXiv:1503.00859.

[13] R. Aaij *et al.* (LHCb Collaboration) Measurement of the time-dependent CP asymmetry in $B^0 \to J/\psi K_S^0$ decays, Phys. Lett. B **721**, 24 (2013).

[14] A. A. Alves, Jr. *et al.* (LHCb Collaboration), The LHCb detector at the LHC, J. Instrum. **3**, S08005 (2008).

[15] R. Aaij *et al.* (LHCb Collaboration) LHCb detector performance, Int. J. Mod. Phys. A **30**, 1530022 (2015).

[16] R. Aaij *et al.*, The LHCb trigger and its performance in 2011, J. Instrum. **8**, P04022 (2013).

[17] K. A. Olive *et al.* (Particle Data Group), Review of particle physics, Chin. Phys. C **38**, 090001 (2014).

[18] W. D. Hulsbergen, Decay chain fitting with a Kalman filter, Nucl. Instrum. Methods Phys. Res., Sect. A **552**, 566 (2005).

[19] T. Sjöstrand, S. Mrenna, and P. Skands, PYTHIA 6.4 physics and manual, J. High Energy Phys. 05 (2006) 026.T. Sjöstrand, S. Mrenna, and P. Skands, A brief introduction to PYTHIA 8.1, Comput. Phys. Commun. **178**, 852 (2008).

[20] I. Belyaev *et al.*, Handling of the generation of primary events in Gauss, the LHCb simulation framework, IEEE Nucl. Sci. Symp. Conf. Rec., 1155 (2010).

[21] D. J. Lange, The EvtGen particle decay simulation package, Nucl. Instrum. Methods Phys. Res., Sect. A **462**, 152 (2001).

[22] J. Allison *et al.* (GEANT4 Collaboration), GEANT4 developments and applications, IEEE Trans. Nucl. Sci. **53**, 270 (2006); S. Agostinelli *et al.* (GEANT4 Collaboration), GEANT4: A simulation toolkit, Nucl. Instrum. Methods Phys. Res., Sect. A **506**, 250 (2003).

[23] M. Clemencic, G. Corti, S. Easo, C. R. Jones, S. Miglioranzi, M. Pappagallo, and P. Robbe, The LHCb simulation application, Gauss: Design, evolution and experience, J. Phys. Conf. Ser. **331**, 032023 (2011).

[24] R. Aaij *et al.* (LHCb Collaboration) Opposite-side flavour tagging of B mesons at the LHCb experiment, Eur. Phys. J. C **72**, 2022 (2012).

[25] M. Gronau, A. Nippe, and J. L. Rosner, Method for flavor tagging in neutral B meson decays, Phys. Rev. D **47**, 1988 (1993).

[26] R. Aaij *et al.* (LHCb Collaboration) Precise measurements of the properties of the $B_1(5721)^{0,+}$ and $B_2^*(5747)^{0,+}$ states and observation of $B^{+,0}\pi^{-,+}$ mass structures, J. High Energy Phys. 04 (2015) 024.

[27] R. Aaij *et al.* (LHCb Collaboration) Measurement of the B^0-$\bar{B}^0$ oscillation frequency Δm_d with the decays $B^0 \to D^-\pi^+$ and $B^0 \to J/\psi K^{*0}$, Phys. Lett. B **719**, 318 (2013).

[28] See Supplemental Material at http://link.aps.org/supplemental/10.1103/PhysRevLett.115.031601 for a summary of the flavor tagging calibration and performance and an overview of the systematic uncertainties.

[29] D. M. Santos and F. Dupertuis, Mass distributions marginalized over per-event errors, Nucl. Instrum. Methods Phys. Res., Sect. A **764**, 150 (2014).

[30] R. Aaij *et al.* (LHCb Collaboration) Measurements of the B^+, B^0, B_s^0 meson and Λ_b^0 baryon lifetimes, J. High Energy Phys. 04 (2014) 114.

[31] R. Aaij *et al.* (LHCb Collaboration) Measurement of the $\bar{B}^0 - B^0$ and $\bar{B}_s^0 - B_s^0$ production asymmetries in pp collisions at $\sqrt{s} = 7$ TeV, Phys. Lett. B **739**, 218 (2014).

[32] R. Aaij *et al.* (LHCb Collaboration) Measurement of the Semileptonic CP Asymmetry in B^0-$\bar{B}^0$ Mixing, Phys. Rev. Lett. **114**, 041601 (2015).

[33] M. Pivk and F. R. Le Diberder, sPlot: A statistical tool to unfold data distributions, Nucl. Instrum. Methods Phys. Res., Sect. A **555**, 356 (2005).

[34] W. Fetscher, P. Kokkas, P. Pavlopoulos, Th. Ruf, and Th. Schietinger, Regeneration of arbitrary coherent neutral kaon states: A new method for measuring the $K^0 - \bar{K}^0$ forward scattering amplitude, Z. Phys. C **72**, 543 (1996); B. R. Ko, E. Won, B. Golob, and P. Pakhlov, Effect of nuclear interactions of neutral kaons on ***CP*** asymmetry measurements, Phys. Rev. D **84**, 111501(R) (2011).

R. Aaij,[41] B. Adeva,[37] M. Adinolfi,[46] A. Affolder,[52] Z. Ajaltouni,[5] S. Akar,[6] J. Albrecht,[9] F. Alessio,[38] M. Alexander,[51] S. Ali,[41] G. Alkhazov,[30] P. Alvarez Cartelle,[53] A. A. Alves Jr.,[57] S. Amato,[2] S. Amerio,[22] Y. Amhis,[7] L. An,[3] L. Anderlini,[17,g] J. Anderson,[40] M. Andreotti,[16,f] J. E. Andrews,[58] R. B. Appleby,[54] O. Aquines Gutierrez,[10] F. Archilli,[38] A. Artamonov,[35] M. Artuso,[59] E. Aslanides,[6] G. Auriemma,[25,n] M. Baalouch,[5] S. Bachmann,[11] J. J. Back,[48] A. Badalov,[36] C. Baesso,[60] W. Baldini,[16,38] R. J. Barlow,[54] C. Barschel,[38] S. Barsuk,[7] W. Barter,[38] V. Batozskaya,[28] V. Battista,[39] A. Bay,[39] L. Beaucourt,[4] J. Beddow,[51] F. Bedeschi,[23] I. Bediaga,[1] L. J. Bel,[41] I. Belyaev,[31] E. Ben-Haim,[8] G. Bencivenni,[18] S. Benson,[38] J. Benton,[46] A. Berezhnoy,[32] R. Bernet,[40] A. Bertolin,[22] M.-O. Bettler,[38] M. van Beuzekom,[41] A. Bien,[11] S. Bifani,[45] T. Bird,[54] A. Birnkraut,[9] A. Bizzeti,[17,i] T. Blake,[48] F. Blanc,[39] J. Blouw,[10] S. Blusk,[59] V. Bocci,[25] A. Bondar,[34] N. Bondar,[30,38] W. Bonivento,[15] S. Borghi,[54] A. Borgia,[59] M. Borsato,[7] T. J. V. Bowcock,[52] E. Bowen,[40] C. Bozzi,[16] S. Braun,[11] D. Brett,[54] M. Britsch,[10] T. Britton,[59] J. Brodzicka,[54] N. H. Brook,[46] A. Bursche,[40] J. Buytaert,[38] S. Cadeddu,[15] R. Calabrese,[16,f] M. Calvi,[20,k] M. Calvo Gomez,[36,p] P. Campana,[18] D. Campora Perez,[38] L. Capriotti,[54] A. Carbone,[14,d] G. Carboni,[24,l] R. Cardinale,[19,j] A. Cardini,[15] P. Carniti,[20] L. Carson,[50] K. Carvalho Akiba,[2,38] R. Casanova Mohr,[36] G. Casse,[52] L. Cassina,[20,k] L. Castillo Garcia,[38] M. Cattaneo,[38] Ch. Cauet,[9] G. Cavallero,[19] R. Cenci,[23,t] M. Charles,[8] Ph. Charpentier,[38] M. Chefdeville,[4] S. Chen,[54] S.-F. Cheung,[55] N. Chiapolini,[40] M. Chrzaszcz,[40,26] X. Cid Vidal,[38] G. Ciezarek,[41] P. E. L. Clarke,[50] M. Clemencic,[38] H. V. Cliff,[47] J. Closier,[38] V. Coco,[38] J. Cogan,[6] E. Cogneras,[5] V. Cogoni,[15,e] L. Cojocariu,[29] G. Collazuol,[22] P. Collins,[38] A. Comerma-Montells,[11] A. Contu,[15,38] A. Cook,[46] M. Coombes,[46] S. Coquereau,[8] G. Corti,[38] M. Corvo,[16,f] I. Counts,[56] B. Couturier,[38] G. A. Cowan,[50] D. C. Craik,[48] A. C. Crocombe,[48] M. Cruz Torres,[60] S. Cunliffe,[53] R. Currie,[53] C. D'Ambrosio,[38] J. Dalseno,[46] P. N. Y. David,[41] A. Davis,[57] K. De Bruyn,[41] S. De Capua,[54] M. De Cian,[11] J. M. De Miranda,[1] L. De Paula,[2] W. De Silva,[57] P. De Simone,[18] C.-T. Dean,[51] D. Decamp,[4] M. Deckenhoff,[9] L. Del Buono,[8] N. Déléage,[4] D. Derkach,[55] O. Deschamps,[5] F. Dettori,[38] B. Dey,[40] A. Di Canto,[38] F. Di Ruscio,[24] H. Dijkstra,[38] S. Donleavy,[52] F. Dordei,[11] M. Dorigo,[39] A. Dosil Suárez,[37] D. Dossett,[48] A. Dovbnya,[43] K. Dreimanis,[52] G. Dujany,[54] F. Dupertuis,[39] P. Durante,[38] R. Dzhelyadin,[35] A. Dziurda,[26] A. Dzyuba,[30] S. Easo,[49,38] U. Egede,[53] V. Egorychev,[31] S. Eidelman,[34] S. Eisenhardt,[50] U. Eitschberger,[9] R. Ekelhof,[9] L. Eklund,[51] I. El Rifai,[5] Ch. Elsasser,[40] S. Ely,[59] S. Esen,[11] H. M. Evans,[47] T. Evans,[55] A. Falabella,[14] C. Färber,[11] C. Farinelli,[41] N. Farley,[45] S. Farry,[52] R. Fay,[52] D. Ferguson,[50] V. Fernandez Albor,[37] F. Ferrari,[14] F. Ferreira Rodrigues,[1] M. Ferro-Luzzi,[38] S. Filippov,[33] M. Fiore,[16,38,f] M. Fiorini,[16,f] M. Firlej,[27] C. Fitzpatrick,[39] T. Fiutowski,[27] P. Fol,[53] M. Fontana,[10]

F. Fontanelli,[19,j] R. Forty,[38] O. Francisco,[2] M. Frank,[38] C. Frei,[38] M. Frosini,[17] J. Fu,[21,38] E. Furfaro,[24,l] A. Gallas Torreira,[37] D. Galli,[14,d] S. Gallorini,[22,38] S. Gambetta,[19,j] M. Gandelman,[2] P. Gandini,[55] Y. Gao,[3] J. García Pardiñas,[37] J. Garofoli,[59] J. Garra Tico,[47] L. Garrido,[36] D. Gascon,[36] C. Gaspar,[38] U. Gastaldi,[16] R. Gauld,[55] L. Gavardi,[9] G. Gazzoni,[5] A. Geraci,[21,v] D. Gerick,[11] E. Gersabeck,[11] M. Gersabeck,[54] T. Gershon,[48] Ph. Ghez,[4] A. Gianelle,[22] S. Gianì,[39] V. Gibson,[47] L. Giubega,[29] V. V. Gligorov,[38] C. Göbel,[60] D. Golubkov,[31] A. Golutvin,[53,31,38] A. Gomes,[1,a] C. Gotti,[20,k] M. Grabalosa Gándara,[5] R. Graciani Diaz,[36] L. A. Granado Cardoso,[38] E. Graugés,[36] E. Graverini,[40] G. Graziani,[17] A. Grecu,[29] E. Greening,[55] S. Gregson,[47] P. Griffith,[45] L. Grillo,[11] O. Grünberg,[63] E. Gushchin,[33] Yu. Guz,[35,38] T. Gys,[38] C. Hadjivasiliou,[59] G. Haefeli,[39] C. Haen,[38] S. C. Haines,[47] S. Hall,[53] B. Hamilton,[58] T. Hampson,[46] X. Han,[11] S. Hansmann-Menzemer,[11] N. Harnew,[55] S. T. Harnew,[46] J. Harrison,[54] J. He,[38] T. Head,[39] V. Heijne,[41] K. Hennessy,[52] P. Henrard,[5] L. Henry,[8] J. A. Hernando Morata,[37] E. van Herwijnen,[38] M. Heß,[63] A. Hicheur,[2] D. Hill,[55] M. Hoballah,[5] C. Hombach,[54] W. Hulsbergen,[41] T. Humair,[53] N. Hussain,[55] D. Hutchcroft,[52] D. Hynds,[51] M. Idzik,[27] P. Ilten,[56] R. Jacobsson,[38] A. Jaeger,[11] J. Jalocha,[55] E. Jans,[41] A. Jawahery,[58] F. Jing,[3] M. John,[55] D. Johnson,[38] C. R. Jones,[47] C. Joram,[38] B. Jost,[38] N. Jurik,[59] S. Kandybei,[43] W. Kanso,[6] M. Karacson,[38] T. M. Karbach,[38] S. Karodia,[51] M. Kelsey,[59] I. R. Kenyon,[45] M. Kenzie,[38] T. Ketel,[42] B. Khanji,[20,38,k] C. Khurewathanakul,[39] S. Klaver,[54] K. Klimaszewski,[28] O. Kochebina,[7] M. Kolpin,[11] I. Komarov,[39] R. F. Koopman,[42] P. Koppenburg,[41,38] M. Korolev,[32] L. Kravchuk,[33] K. Kreplin,[11] M. Kreps,[48] G. Krocker,[11] P. Krokovny,[34] F. Kruse,[9] W. Kucewicz,[26,o] M. Kucharczyk,[26] V. Kudryavtsev,[34] K. Kurek,[28] T. Kvaratskheliya,[31] V. N. La Thi,[39] D. Lacarrere,[38] G. Lafferty,[54] A. Lai,[15] D. Lambert,[50] R. W. Lambert,[42] G. Lanfranchi,[18] C. Langenbruch,[48] B. Langhans,[38] T. Latham,[48] C. Lazzeroni,[45] R. Le Gac,[6] J. van Leerdam,[41] J.-P. Lees,[4] R. Lefèvre,[5] A. Leflat,[32] J. Lefrançois,[7] O. Leroy,[6] T. Lesiak,[26] B. Leverington,[11] Y. Li,[7] T. Likhomanenko,[64] M. Liles,[52] R. Lindner,[38] C. Linn,[38] F. Lionetto,[40] B. Liu,[15] S. Lohn,[38] I. Longstaff,[51] J. H. Lopes,[2] P. Lowdon,[40] D. Lucchesi,[22,r] H. Luo,[50] A. Lupato,[22] E. Luppi,[16,f] O. Lupton,[55] F. Machefert,[7] I. V. Machikhiliyan,[31] F. Maciuc,[29] O. Maev,[30] S. Malde,[55] A. Malinin,[64] G. Manca,[15,e] G. Mancinelli,[6] P. Manning,[59] A. Mapelli,[38] J. Maratas,[5] J. F. Marchand,[4] U. Marconi,[14] C. Marin Benito,[36] P. Marino,[23,38,t] R. Märki,[39] J. Marks,[11] G. Martellotti,[25] M. Martinelli,[39] D. Martinez Santos,[42] F. Martinez Vidal,[66] D. Martins Tostes,[2] A. Massafferri,[1] R. Matev,[38] Z. Mathe,[38] C. Matteuzzi,[20] A. Mauri,[40] B. Maurin,[39] A. Mazurov,[45] M. McCann,[53] J. McCarthy,[45] A. McNab,[54] R. McNulty,[12] B. McSkelly,[52] B. Meadows,[57] F. Meier,[9] M. Meissner,[11] M. Merk,[41] D. A. Milanes,[62] M.-N. Minard,[4] D. S. Mitzel,[11] J. Molina Rodriguez,[60] S. Monteil,[5] M. Morandin,[22] P. Morawski,[27] A. Mordà,[6] M. J. Morello,[23,t] J. Moron,[27] A.-B. Morris,[50] R. Mountain,[59] F. Muheim,[50] K. Müller,[40] V. Müller,[9] M. Mussini,[14] B. Muster,[39] P. Naik,[46] T. Nakada,[39] R. Nandakumar,[49] I. Nasteva,[2] M. Needham,[50] N. Neri,[21] S. Neubert,[11] N. Neufeld,[38] M. Neuner,[11] A. D. Nguyen,[39] T. D. Nguyen,[39] C. Nguyen-Mau,[39,q] V. Niess,[5] R. Niet,[9] N. Nikitin,[32] T. Nikodem,[11] A. Novoselov,[35] D. P. O'Hanlon,[48] A. Oblakowska-Mucha,[27] V. Obraztsov,[35] S. Ogilvy,[51] O. Okhrimenko,[44] R. Oldeman,[15,e] C. J. G. Onderwater,[67] B. Osorio Rodrigues,[1] J. M. Otalora Goicochea,[2] A. Otto,[38] P. Owen,[53] A. Oyanguren,[66] A. Palano,[13,c] F. Palombo,[21,u] M. Palutan,[18] J. Panman,[38] A. Papanestis,[49] M. Pappagallo,[51] L. L. Pappalardo,[16,f] C. Parkes,[54] G. Passaleva,[17] G. D. Patel,[52] M. Patel,[53] C. Patrignani,[19,j] A. Pearce,[54,49] A. Pellegrino,[41] G. Penso,[25,m] M. Pepe Altarelli,[38] S. Perazzini,[14,d] P. Perret,[5] L. Pescatore,[45] K. Petridis,[46] A. Petrolini,[19,j] E. Picatoste Olloqui,[36] B. Pietrzyk,[4] T. Pilař,[48] D. Pinci,[25] A. Pistone,[19] S. Playfer,[50] M. Plo Casasus,[37] T. Poikela,[38] F. Polci,[8] A. Poluektov,[48,34] I. Polyakov,[31] E. Polycarpo,[2] A. Popov,[35] D. Popov,[10] B. Popovici,[29] C. Potterat,[2] E. Price,[46] J. D. Price,[52] J. Prisciandaro,[39] A. Pritchard,[52] C. Prouve,[46] V. Pugatch,[44] A. Puig Navarro,[39] G. Punzi,[23,s] W. Qian,[4] R. Quagliani,[7,46] B. Rachwal,[26] J. H. Rademacker,[46] B. Rakotomiaramanana,[39] M. Rama,[23] M. S. Rangel,[2] I. Raniuk,[43] N. Rauschmayr,[38] G. Raven,[42] F. Redi,[53] S. Reichert,[54] M. M. Reid,[48] A. C. dos Reis,[1] S. Ricciardi,[49] S. Richards,[46] M. Rihl,[38] K. Rinnert,[52] V. Rives Molina,[36] P. Robbe,[7,38] A. B. Rodrigues,[1] E. Rodrigues,[54] J. A. Rodriguez Lopez,[62] P. Rodriguez Perez,[54] S. Roiser,[38] V. Romanovsky,[35] A. Romero Vidal,[37] M. Rotondo,[22] J. Rouvinet,[39] T. Ruf,[38] H. Ruiz,[36] P. Ruiz Valls,[66] J. J. Saborido Silva,[37] N. Sagidova,[30] P. Sail,[51] B. Saitta,[15,e] V. Salustino Guimaraes,[2] C. Sanchez Mayordomo,[66] B. Sanmartin Sedes,[37] R. Santacesaria,[25] C. Santamarina Rios,[37] E. Santovetti,[24,l] A. Sarti,[18,m] C. Satriano,[25,n] A. Satta,[24] D. M. Saunders,[46] D. Savrina,[31,32] M. Schellenberg,[9] M. Schiller,[38] H. Schindler,[38] M. Schlupp,[9] M. Schmelling,[10] B. Schmidt,[38] O. Schneider,[39] A. Schopper,[38] M.-H. Schune,[7] R. Schwemmer,[38] B. Sciascia,[18] A. Sciubba,[25,m] A. Semennikov,[31] I. Sepp,[53] N. Serra,[40] J. Serrano,[6] L. Sestini,[22] P. Seyfert,[11] M. Shapkin,[35] I. Shapoval,[16,43,f] Y. Shcheglov,[30] T. Shears,[52] L. Shekhtman,[34] V. Shevchenko,[64] A. Shires,[9] R. Silva Coutinho,[48] G. Simi,[22] M. Sirendi,[47] N. Skidmore,[46] I. Skillicorn,[51] T. Skwarnicki,[59] N. A. Smith,[52] E. Smith,[55,49] E. Smith,[53] J. Smith,[47] M. Smith,[54] H. Snoek,[41] M. D. Sokoloff,[57,38] F. J. P. Soler,[51] F. Soomro,[39] D. Souza,[46] B. Souza De Paula,[2] B. Spaan,[9] P. Spradlin,[51] S. Sridharan,[38]

F. Stagni,[38] M. Stahl,[11] S. Stahl,[38] O. Steinkamp,[40] O. Stenyakin,[35] F. Sterpka,[59] S. Stevenson,[55] S. Stoica,[29] S. Stone,[59] B. Storaci,[40] S. Stracka,[23,t] M. Straticiuc,[29] U. Straumann,[40] R. Stroili,[22] L. Sun,[57] W. Sutcliffe,[53] K. Swientek,[27] S. Swientek,[9] V. Syropoulos,[42] M. Szczekowski,[28] P. Szczypka,[39,38] T. Szumlak,[27] S. T'Jampens,[4] M. Teklishyn,[7] G. Tellarini,[16,f] F. Teubert,[38] C. Thomas,[55] E. Thomas,[38] J. van Tilburg,[41] V. Tisserand,[4] M. Tobin,[39] J. Todd,[57] S. Tolk,[42] L. Tomassetti,[16,f] D. Tonelli,[38] S. Topp-Joergensen,[55] N. Torr,[55] E. Tournefier,[4] S. Tourneur,[39] K. Trabelsi,[39] M. T. Tran,[39] M. Tresch,[40] A. Trisovic,[38] A. Tsaregorodtsev,[6] P. Tsopelas,[41] N. Tuning,[41,38] M. Ubeda Garcia,[38] A. Ukleja,[28] A. Ustyuzhanin,[65] U. Uwer,[11] C. Vacca,[15,e] V. Vagnoni,[14] G. Valenti,[14] A. Vallier,[7] R. Vazquez Gomez,[18] P. Vazquez Regueiro,[37] C. Vázquez Sierra,[37] S. Vecchi,[16] J. J. Velthuis,[46] M. Veltri,[17,h] G. Veneziano,[39] M. Vesterinen,[11] J. V. Viana Barbosa,[38] B. Viaud,[7] D. Vieira,[2] M. Vieites Diaz,[37] X. Vilasis-Cardona,[36,p] A. Vollhardt,[40] D. Volyanskyy,[10] D. Voong,[46] A. Vorobyev,[30] V. Vorobyev,[34] C. Voß,[63] J. A. de Vries,[41] R. Waldi,[63] C. Wallace,[48] R. Wallace,[12] J. Walsh,[23] S. Wandernoth,[11] J. Wang,[59] D. R. Ward,[47] N. K. Watson,[45] D. Websdale,[53] A. Weiden,[40] M. Whitehead,[48] D. Wiedner,[11] G. Wilkinson,[55,38] M. Wilkinson,[59] M. Williams,[38] M. P. Williams,[45] M. Williams,[56] F. F. Wilson,[49] J. Wimberley,[58] J. Wishahi,[9] W. Wislicki,[28] M. Witek,[26] G. Wormser,[7] S. A. Wotton,[47] S. Wright,[47] K. Wyllie,[38] Y. Xie,[61] Z. Xu,[39] Z. Yang,[3] X. Yuan,[34] O. Yushchenko,[35] M. Zangoli,[14] M. Zavertyaev,[10,b] L. Zhang,[3] Y. Zhang,[3] A. Zhelezov,[11] A. Zhokhov,[31] and L. Zhong[3]

(LHCb collaboration)

[1]*Centro Brasileiro de Pesquisas Físicas (CBPF), Rio de Janeiro, Brazil*
[2]*Universidade Federal do Rio de Janeiro (UFRJ), Rio de Janeiro, Brazil*
[3]*Center for High Energy Physics, Tsinghua University, Beijing, China*
[4]*LAPP, Université Savoie Mont-Blanc, CNRS/IN2P3, Annecy-Le-Vieux, France*
[5]*Clermont Université, Université Blaise Pascal, CNRS/IN2P3, LPC, Clermont-Ferrand, France*
[6]*CPPM, Aix-Marseille Université, CNRS/IN2P3, Marseille, France*
[7]*LAL, Université Paris-Sud, CNRS/IN2P3, Orsay, France*
[8]*LPNHE, Université Pierre et Marie Curie, Université Paris Diderot, CNRS/IN2P3, Paris, France*
[9]*Fakultät Physik, Technische Universität Dortmund, Dortmund, Germany*
[10]*Max-Planck-Institut für Kernphysik (MPIK), Heidelberg, Germany*
[11]*Physikalisches Institut, Ruprecht-Karls-Universität Heidelberg, Heidelberg, Germany*
[12]*School of Physics, University College Dublin, Dublin, Ireland*
[13]*Sezione INFN di Bari, Bari, Italy*
[14]*Sezione INFN di Bologna, Bologna, Italy*
[15]*Sezione INFN di Cagliari, Cagliari, Italy*
[16]*Sezione INFN di Ferrara, Ferrara, Italy*
[17]*Sezione INFN di Firenze, Firenze, Italy*
[18]*Laboratori Nazionali dell'INFN di Frascati, Frascati, Italy*
[19]*Sezione INFN di Genova, Genova, Italy*
[20]*Sezione INFN di Milano Bicocca, Milano, Italy*
[21]*Sezione INFN di Milano, Milano, Italy*
[22]*Sezione INFN di Padova, Padova, Italy*
[23]*Sezione INFN di Pisa, Pisa, Italy*
[24]*Sezione INFN di Roma Tor Vergata, Roma, Italy*
[25]*Sezione INFN di Roma La Sapienza, Roma, Italy*
[26]*Henryk Niewodniczanski Institute of Nuclear Physics Polish Academy of Sciences, Kraków, Poland*
[27]*AGH-University of Science and Technology, Faculty of Physics and Applied Computer Science, Kraków, Poland*
[28]*National Center for Nuclear Research (NCBJ), Warsaw, Poland*
[29]*Horia Hulubei National Institute of Physics and Nuclear Engineering, Bucharest-Magurele, Romania*
[30]*Petersburg Nuclear Physics Institute (PNPI), Gatchina, Russia*
[31]*Institute of Theoretical and Experimental Physics (ITEP), Moscow, Russia*
[32]*Institute of Nuclear Physics, Moscow State University (SINP MSU), Moscow, Russia*
[33]*Institute for Nuclear Research of the Russian Academy of Sciences (INR RAN), Moscow, Russia*
[34]*Budker Institute of Nuclear Physics (SB RAS) and Novosibirsk State University, Novosibirsk, Russia*
[35]*Institute for High Energy Physics (IHEP), Protvino, Russia*
[36]*Universitat de Barcelona, Barcelona, Spain*
[37]*Universidad de Santiago de Compostela, Santiago de Compostela, Spain*
[38]*European Organization for Nuclear Research (CERN), Geneva, Switzerland*

[39]Ecole Polytechnique Fédérale de Lausanne (EPFL), Lausanne, Switzerland
[40]Physik-Institut, Universität Zürich, Zürich, Switzerland
[41]Nikhef National Institute for Subatomic Physics, Amsterdam, The Netherlands
[42]Nikhef National Institute for Subatomic Physics and VU University Amsterdam, Amsterdam, The Netherlands
[43]NSC Kharkiv Institute of Physics and Technology (NSC KIPT), Kharkiv, Ukraine
[44]Institute for Nuclear Research of the National Academy of Sciences (KINR), Kyiv, Ukraine
[45]University of Birmingham, Birmingham, United Kingdom
[46]H.H. Wills Physics Laboratory, University of Bristol, Bristol, United Kingdom
[47]Cavendish Laboratory, University of Cambridge, Cambridge, United Kingdom
[48]Department of Physics, University of Warwick, Coventry, United Kingdom
[49]STFC Rutherford Appleton Laboratory, Didcot, United Kingdom
[50]School of Physics and Astronomy, University of Edinburgh, Edinburgh, United Kingdom
[51]School of Physics and Astronomy, University of Glasgow, Glasgow, United Kingdom
[52]Oliver Lodge Laboratory, University of Liverpool, Liverpool, United Kingdom
[53]Imperial College London, London, United Kingdom
[54]School of Physics and Astronomy, University of Manchester, Manchester, United Kingdom
[55]Department of Physics, University of Oxford, Oxford, United Kingdom
[56]Massachusetts Institute of Technology, Cambridge, Massachusetts, USA
[57]University of Cincinnati, Cincinnati, Ohio, USA
[58]University of Maryland, College Park, Maryland, USA
[59]Syracuse University, Syracuse, New York, USA
[60]Pontifícia Universidade Católica do Rio de Janeiro (PUC-Rio), Rio de Janeiro, Brazil,
associated with (Universidade Federal do Rio de Janeiro (UFRJ), Rio de Janeiro, Brazil)
[61]Institute of Particle Physics, Central China Normal University, Wuhan, Hubei, China,
associated with (Center for High Energy Physics, Tsinghua University, Beijing, China)
[62]Departamento de Fisica, Universidad Nacional de Colombia, Bogota, Colombia,
associated with (LPNHE, Université Pierre et Marie Curie, Université Paris Diderot, CNRS/IN2P3, Paris, France)
[63]Institut für Physik, Universität Rostock, Rostock, Germany,
associated with (Physikalisches Institut, Ruprecht-Karls-Universität Heidelberg, Heidelberg, Germany)
[64]National Research Centre Kurchatov Institute, Moscow, Russia,
associated with (Institute of Theoretical and Experimental Physics (ITEP), Moscow, Russia)
[65]Yandex School of Data Analysis, Moscow, Russia,
associated with (Institute of Theoretical and Experimental Physics (ITEP), Moscow, Russia)
[66]Instituto de Fisica Corpuscular (IFIC), Universitat de Valencia-CSIC, Valencia, Spain,
associated with (Universitat de Barcelona, Barcelona, Spain)
[67]Van Swinderen Institute, University of Groningen, Groningen, The Netherlands,
associated with (Nikhef National Institute for Subatomic Physics, Amsterdam, The Netherlands)

[a]Universidade Federal do Triângulo Mineiro (UFTM), Uberaba-MG, Brazil.
[b]P.N. Lebedev Physical Institute, Russian Academy of Science (LPI RAS), Moscow, Russia.
[c]Università di Bari, Bari, Italy.
[d]Università di Bologna, Bologna, Italy.
[e]Università di Cagliari, Cagliari, Italy.
[f]Università di Ferrara, Ferrara, Italy.
[g]Università di Firenze, Firenze, Italy
[h]Università di Urbino, Urbino, Italy.
[I]Università di Modena e Reggio Emilia, Modena, Italy.
[j]Università di Genova, Genova, Italy.
[k]Università di Milano Bicocca, Milano, Italy.
[l]Università di Roma Tor Vergata, Roma, Italy.
[m]Università di Roma La Sapienza, Roma, Italy.
[n]Università della Basilicata, Potenza, Italy.
[o]AGH-University of Science and Technology, Faculty of Computer Science, Electronics and Telecommunications, Kraków, Poland.
[p]LIFAELS, La Salle, Universitat Ramon Llull, Barcelona, Spain.
[q]Hanoi University of Science, Hanoi, Viet Nam.
[r]Università di Padova, Padova, Italy.
[s]Università di Pisa, Pisa, Italy.
[t]Scuola Normale Superiore, Pisa, Italy.
[u]Università degli Studi di Milano, Milano, Italy.
[v]Politecnico di Milano, Milano, Italy.